https://doi.org/10.32603/1993-8985-2019-22-3-48-62
УДК 621.396.677.85

Andrey V. Mozharovskiy ✉
LLC "Radio Gigabit"
95, bldg 2, Osharskaya Str., 603105, Nishny Novgorod, Russia

DESIGN OF LENS ANTENNA WITH PLANAR ORTHOMODE TRANSDUCER FOR 28 GHZ FIXED SERVICE COMMUNICATION SYSTEMS

Abstract.
Introduction*. Due to its support for the utilisation of wide transmission frequency bands, the millimetre-wave frequency range can significantly increase the capacity of modern communication systems. However, one of the current problems affecting the design of the 27.5…29.5 GHz-wave communication system is the design of a high gain antenna of the range of 30 dBi to compensate for the significant level of radio signal attenuation in the communication channel compared to traditional frequency bands below 6 GHz.*
Objective. *The research aims at the development an integrated lens antenna with the capability of operating on two orthogonal linear polarisations in order to create more efficient use of the spectrum by separating the transmitted and received signals by polarisation. An additional important task is to provide a high aperture efficiency of the antenna and a low level of insertion loss in the distribution system, which should have an interface based on printed transmission lines for connection to the radio frequency circuit elements realised on a printed circuit board.*
Materials and methods. *The main method for analysing the lens antenna characteristics is full-wave electromagnetic simulation in the CST Microwave Studio computer-aided design system. The results are confirmed by means of experimental sample measurement.*
Results. *The designed antenna comprises an integrated lens antenna consisting of a homogeneous semi-elliptical dielectric lens with a diameter of D = 120 mm with a cylindrical extension and a primary radiator based on a microstrip antenna with a waveguide adapter. The radiating opening dimensions of the waveguide adapter were optimised using an analytical method based on a combination of geometrical and physical optics. Two orthogonal polarisations were excited on the primary microstrip patch antenna with the corresponding closely spaced "H-type" slots in one internal metallisation layer. According to experimental results, the designed antenna provides the gain level of 29.5–30.2 dBi having a half-power beamwidth of 4.8–5.1 degrees and a cross-polarisation level exceeding 37 dB for both polarisations across the whole frequency band of 27.5–29.5 GHz.*
Conclusion. *Due to the simplicity of the design, high aperture efficiency and the ability to operate on two orthogonal linear polarisations, the developed lens antenna can be successfully used in radio communication systems of the 27.5…29.5 GHz frequency range.*

Keywords: millimetre wave band, integrated lens antenna, microstrip antenna, printed circuit board, waveguide-to-microstrip transition, dual linear polarisation, EM simulation

For citation: Mozharovskiy A. V. Design of Lens Antenna with Planar Orthomode Transducer for 28 GHz RADIO COMMUNICATION SYSTEMs. Journal of the Russian Universities. Radioelectronics. 2019, vol. 22, no. 3, pp. 48–62. doi: 10.32603/1993-8985-2019-22-3-48-62

Acknowledgements. Initiative work.

Conflict of interest. The authors declare no conflict of interest.

Submitted 12.04.2019; accepted 20.05.2019; published online 27.06.2019

А. В. Можаровский ✉
ООО "Радио Гигабит"
ул. Ошарская, 95 к. 2, Нижний Новгород, 603105, Россия

РАЗРАБОТКА ЛИНЗОВОЙ АНТЕННЫ С ПЛАНАРНЫМ ПОЛЯРИЗАЦИОННЫМ СЕЛЕКТОРОМ ДЛЯ СИСТЕМ ФИКСИРОВАННОЙ РАДИОСВЯЗИ ЧАСТОТНОГО ДИАПАЗОНА 28 ГГЦ

Аннотация

Введение. *Использование миллиметрового диапазона длин волн открывает широкие перспективы для увеличения пропускной способности в современных системах связи за счет применения широких полос передаваемых сигналов. Одной из основных сложностей при разработке систем радиосвязи диапазона длин волн 27.5...29.5 ГГц является обеспечение высоких значений коэффициента усиления используемых антенн порядка 30 дБи для компенсации значительного уровня затухания радиосигнала в канале связи по сравнению с традиционными диапазонами частот ниже 6 ГГц.*

Цель работы. *Разработка узконаправленной антенны с возможностью работы на двух ортогональных линейных поляризациях для разделения передаваемого и принимаемого потоков по поляризации и, соответственно, более эффективного использования спектра. При этом важной задачей является обеспечение высокой апертурной эффективности антенны и низкий уровень потерь в системе подведения, которая должна иметь интерфейс на основе печатных линий передачи для подключения к элементам радиочастотного тракта, реализованным на печатной плате.*

Материалы и методы. *Основным методом исследования характеристик антенны является численное электродинамическое моделирование в системе автоматизированного проектирования CST Microwave Studio. Полученные результаты подтверждены при измерении экспериментальных образцов.*

Результаты. *В качестве разрабатываемой антенны выбрана интегрированная линзовая антенна, состоящая из однородной полуэллиптической диэлектрической линзы диаметром D = 120 мм с цилиндрическим продолжением и первичного облучателя, выполненного на основе микрополосковой антенны с волноводным адаптером. Размер раскрыва адаптера оптимизирован для увеличения апертурной эффективности линзы с помощью комбинированного метода на основе принципов геометрической и физической оптики. Две ортогональные линейные поляризации на микрополосковом облучателе возбуждаются через соответствующие щели "H"-формы, выполненные в одном из внутренних уровней металлизации печатной платы рядом друг с другом. В частотном диапазоне 27.5...29.5 ГГц разработанная линзовая антенна для каждой из поляризаций обеспечивает значение коэффициента усиления 29.5...30.2 дБи с шириной основного луча по уровню половинной мощности 4.8...5.1° и уровнем кроссполяризационной развязки не менее 37 дБ.*

Заключение. *Простота конструкции, высокая апертурная эффективность и возможность работать на двух ортогональных линейных поляризациях позволяют сделать вывод, что разработанная линзовая антенна может быть успешно использована в системах радиосвязи частотного диапазона 27.5...29.5 ГГц.*

Ключевые слова: миллиметровый диапазон длин волн, интегрированная линзовая антенна, микрополосковая антенна, печатная плата, волноводно-микрополосковый переход, двойная линейная поляризация, электродинамическое моделирование

Для цитирования: Можаровский А. В. Разработка линзовой антенны с планарным поляризационным селектором для систем фиксированной радиосвязи частотного диапазона 28 ГГц // Изв. вузов России. Радиоэлектроника. 2019. Т. 22, № 3. С. 48–62. doi: 10.32603/1993-8985-2019-22-3-48-62

Источник финансирования. Инициативная работа.

Конфликт интересов. Авторы заявляют об отсутствии конфликта интересов.

Статья поступила в редакцию 12.04.2019; принята к публикации 20.05.2019; опубликована онлайн 27.06.2019

Introduction. The rapid growth in the volume of information transmitted across modern wireless networks results in the necessity for a significant increase in the capacity of communication systems and consequent increase of a data transmission speeds exceeding several gigabits per second. To achieve such speeds, it is necessary to use a wide transmission band; however, this proves extremely challeng-

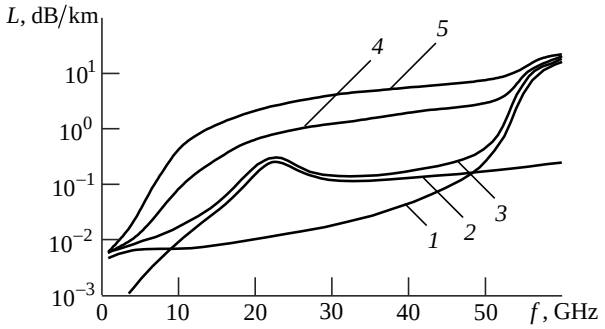

Fig. 1. Radio signal attenuation level in a communication channel caused by oxygen, water vapor and precipitation

ing in the overloaded frequency spectrum bands below 6 GHz traditionally used in radio communications. A possible solution consists in an increase of the carrier frequency up to the so-called millimetre-wave range, where frequency bands up to several gigahertz are available for data transmission. Presently, the frequency band between 27.5…29.5 GHz is considered as one of the most promising for implementation of "point-to-point" and "point-to-multipoint" wireless communication systems [1]–[3], as well as for the deployment of fifth generation (5G) mobile networks [4].

One of the main developmental challenges in millimetre-wave frequency range radio communication systems is to provide high antenna gain values (AG) in order to compensate for the significant level of radio signal attenuation in communication channels relative to the frequency bands below 6 GHz. The main reason for signal attenuation (L) in a radio communications channel consists in the influence of oxygen and water vapour [5]–[7], as is shown for various frequencies f in Fig. 1 (Curve 1 denotes oxygen, Curve 2 denotes water vapour, Curve 3 is for clear conditions, Curve 4 is for rainfall of 5 mm/h, while Curve 5 is for rain of 20 mm/h).

In addition, as shown in [6], [8], and explained in the International Telecommunication Union (ITU) recommendations [9], precipitation significantly increases attenuation level. Should the precipitation intensity correspond to heavy rain, overall signal attenuation increases from 0.05 dB/km to 6 dB/km when an operating frequency increases from 6 GHz to 28.5 GHz (the centre of the considered frequency band) (Fig. 1), which significantly affects radio channel characteristics. In this regard, the principal regulatory documents applying in the Russian Federation and European countries authorise the use of a high gain antenna in a frequency range around 28 GHz for point-to-point communication systems and a combination of narrow-beam subscriber unit antenna and single-beam sector base station antenna for point-to-multipoint systems.

At the same time, rain intensity is a statistical parameter having a certain probability density specific to each geographical area [10]. Typically, channel availability is selected as a criterion for the evaluation of a communication system in order to determine the average declared full capacity time. In modern communication systems availability criteria of 99.9, 99.99 and 99.999% are generally used, corresponding to an absence of connection in the selected channel for approximately 52 minutes, 5 minutes and 30 seconds per year, respectively. The communication range can be calculated by using the classical Friis transmission equation in which losses affecting propagation of radio signal in atmospheric gases and losses due to rain are taken into account:

$$P_{\mathrm{r}} - P_{\mathrm{t}} = 20\lg\left(\frac{\lambda}{4\pi R}\right) + G_{\mathrm{r}} + G_{\mathrm{t}} - \\ -R\left(\gamma_{\mathrm{oxygen}} + \gamma_{\mathrm{vapor}} + \gamma_{\mathrm{rain}}\right),$$

where P_{r} and P_{t} are received and transmitted powers, respectively, in dBm; λ is a radiation wavelength (10.53 mm for a frequency of 28.5 GHz); R is a communication range; G_{r} and G_{t} are the respective gains of the receiving and transmitting antennas; $\gamma_{\mathrm{oxygen}}, \gamma_{\mathrm{vapor}}, \gamma_{\mathrm{rain}}$ correspond to signal attenuation coefficients in oxygen, water vapour and rain, respectively. The attenuation coefficients for frequencies from 1 to 1000 GHz are reported in [7] and [9].

According to calculations, a link distance of over 4 km can only be achieved on the lowest modulations in case of availability criteria of 99.99% in a precipitation zone corresponding to Central Russia using antennas providing AG of 30 dBi and higher. These AG values correspond to an aperture size of about 120 mm in the considered frequency band. The selected geographic area is located in the temperate zone with an average level of precipitation per year. Therefore, obtained results can be considered as an average over the geographical location of the most populated parts of the continents.

Additionally, in order to ensure efficient utilisation of the spectrum, it is possible to implement a communications system using MIMO (Multiple Input Multiple Output) technology [11], which allows simultaneous parallel transmission of several data streams using several antennas and separation by polarisation.

Thus, the purpose of the present research is to develop an effective antenna with a high AG level for

radio communication systems in the 27.5…29.5 GHz frequency band, which is capable of operating on two orthogonal linear polarisations to ensure efficient separation of received and transmitted signals by polarisation. Since the antenna is designed as a part of communication systems, an important requirement is an output interface based on a printed transmission line for direct connection to radio frequency circuit elements, such as low-noise amplifiers (LNA), mixers and filters. Another important issue when developing a millimetre-wave high gain antenna is ensuring a high antenna aperture efficiency and low-loss feed system, since printed structure losses increase significantly when the operating frequency is increased to the millimetre-wave range. Therefore, it is necessary to analyse the principles according to which the efficiency of the high gain antenna aperture can be maximised.

The main antenna requirements are a high AG (around 30 dBi), the ability to work on two orthogonal linear polarisations with a cross-polarisation level of more than 30 dB and a reflection coefficient level of $S_{11} < -10$ dB in the considered frequency band of 27.5…29.5 GHz.

Antenna configuration. There are various approaches to the design of a high gain antenna that supports operation on two orthogonal linear polarisations in the millimetre-wave frequency range. For example, a promising planar solution having low mass-production costs can be realised on a two-dimensional array of printed microstrip antenna elements [12]–[14]. However, in order to ensure a high AG value, this array must contain a large number of antenna elements, significantly complicating the signal distribution system and consequently increasing losses up to several decibels, especially when using two polarisations.

Losses in the signal distribution system can be significantly reduced by using a series feed circuit comprised of antenna array elements [15]–[16], which can additionally be implemented using substrate integrated waveguide (SIW) [17] technology. The main disadvantage of using a series feed circuit is the frequency dependence of the main radiation pattern lobe direction, which is caused by a change in a phase shift between adjacent array elements when changing an operating frequency. A possible approach to solving this problem consists in symmetric excitation of signal distribution system branches [18]–[19]. In this case, opposite branches allow the lobe oscillation to be compensated when the frequency changes; however, this leads to a decrease in AG which limits this solution to a relatively narrow band.

Another approach to reducing losses in the signal distribution system of a two-dimensional antenna array is an implementation based on hollow metal waveguides [20]. In this case, the antenna elements can be comprised of slot- or small horn antennas. The main disadvantage of this approach is the bulkiness of the waveguide elements in the considered frequency range, the complexity of their manufacture and the additional requirement of a solution to the problem of transition from a waveguide interface to a printed transmission line for integration with a radio frequency module.

A Cassegrain antenna, which employs a dual-polarised primary feed [21], can also be considered as a reflector antenna solution. This approach is widely used in commercial implementations of high gain antennas of the considered frequency range due to their relatively simple design and use of a standard circular or square metal waveguide interface. Nevertheless, commercial solutions based on this approach tend to be expensive. One of the drawbacks of this antenna type is the radiating aperture shadowing effect caused by the secondary reflector. At the same time, since the size of the secondary reflector typically changes slightly with an increase in the size of the parabolic reflector (and, accordingly, with AG increase), the shadowing effect is more critical for antennas having a moderate AG value, such as those considered in this article.

Under the present research framework, an integrated lens antenna (ILA) [22]–[24] was selected as the basic approach for the implementation of a dual-polarised high-gain antenna in the frequency range of 27.5…29.5 GHz. This choice is due to a number of well-known advantages of ILA in comparison with other aperture antennas. In particular, they have no aperture shadowing effect (unlike Cassegrain antennas), and there is also a possibility of a primary radiator implementation on a printed circuit board together with radio frequency circuit elements that greatly simplifies the communication systems development.

An ILA generally consists of a homogeneous dielectric lens having an elliptical (or quasi-elliptical) shape with a primary radiator located in its focus. Proceeding from geometric optics laws, it can be seen that if an ellipsoid eccentricity e satisfies the relation $e = 1/n$, where n is a lens material refractive index, then both the geometric and optical foci of an ellipsoid coincide. In this case, the primary feed radi-

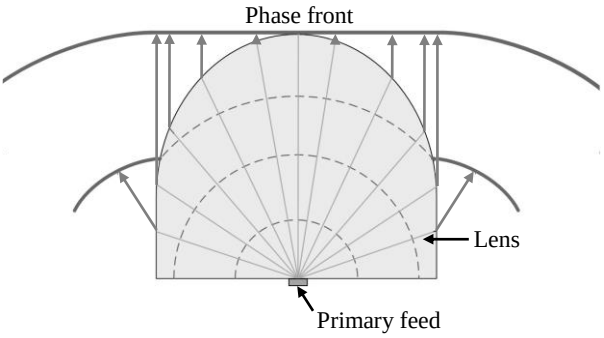

Fig. 2. The primary feed rays path and phase front

ation passes through a "dielectric–empty space" interface forming a planar phase front and, accordingly, a narrow beam of a radiation pattern (RP) in a far field (Fig. 2). Thus, the focusing principle of an ILA is similar to that in classical reflector antennas and thin lenses having a remote primary radiator. Since the bottom part of the lens (cylindrical extension) does not participate in the focusing of radiation, its shape can be arbitrarily modified to integrate the lens antenna with the radio relay station housing.

The designed antenna consists of a hemielliptical lens with a diameter of D=120 mm. It is made of a high-density polyethylene (HDPE) with a dielectric constant of $\varepsilon = 2.3$ and a low loss tangent value $\left(\mathrm{tg}\,\delta = 2\cdot 10^{-4}\right)$ in the considered frequency band. The primary lens feed is located on a flat lens base at the focal point, as shown in Fig. 3.

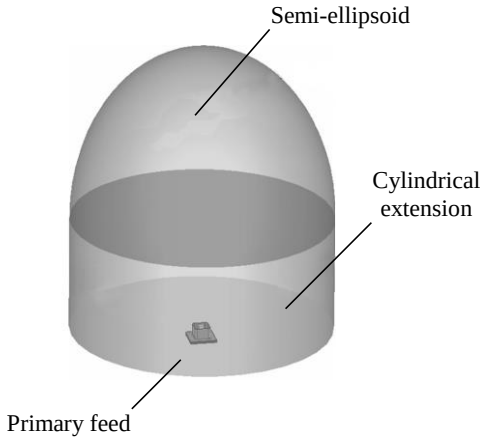

Fig. 3. Lens antenna model

Primary feed design and characteristics. An important task in the high gain ILA design is to provide effective illumination of the collimating elliptical lens surface by means of the primary feed [23], [25], [26]. The amplitude distribution is determined by the radiation pattern shape of the primary feed on the radiating surface of the lens body and, consequently, the ILA radiation pattern shape and AG value in the far field. Thus, if the primary feed has a wide radiation pattern in the lens body, then a significant part of radiated power is used to illuminate the cylindrical extension, which does not participate in an ILA radiation pattern narrow beam formation (Fig. 4, *a*). This leads to an increase in the radiation pattern of the side and back lobes and a reduction in the amplitude of the main lobe.

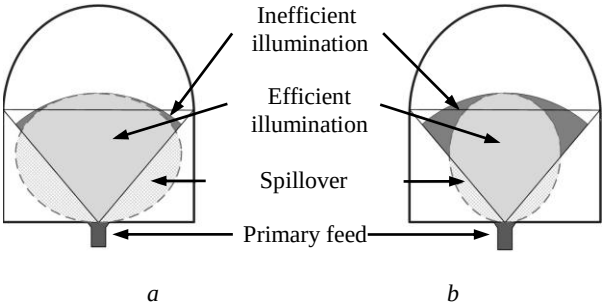

Fig. 4. Lens collimating surface illumination by the primary feed

Conversely, if the primary feed has a narrow radiation pattern, then its radiated power is concentrated in the centre of the elliptical part of the lens reducing its effective radiating aperture and antenna gain (Fig. 4, *b*). Thus, it is possible to provide a more effective illumination of the elliptical surface of the lens and, accordingly, increase ILA AG by controlling the width of the primary feed radiation pattern.

In order to determine the fundamental dependence of the ILA antenna directivity (AD) on a RP width of its primary feed at a half-power beamwidth, the specialised MATLAB software is used to calculate the ILA characteristics. The calculation method is based on a hybrid method combining the principles of geometrical and physical optics (GO/PO) [27]. In this case, the primary feed radiation pattern within the lens body is considered axisymmetric, while the angular distribution of the electric field amplitude is determined as:

$$\left|\vec{E}_{\text{p.f}}(\theta)\right| = E_0 \cos^{\gamma}(\theta),$$

where E_0 is the main lobe amplitude; θ is the angle measured from the lens axis; γ is the coefficient that determines the primary feed radiation pattern width in the lens body. The calculation results for an HDPE lens with a diameter of D = 120 mm at a band centre frequency of 28.5 GHz are shown in Fig. 5.

From the figure it follows that the primary feed with a radiation pattern width of 44…50° provides the maximum AD value for the selected lens type – and, therefore, AG. It is noted that the width of the primary feed radiation pattern that provides the maximum ILA

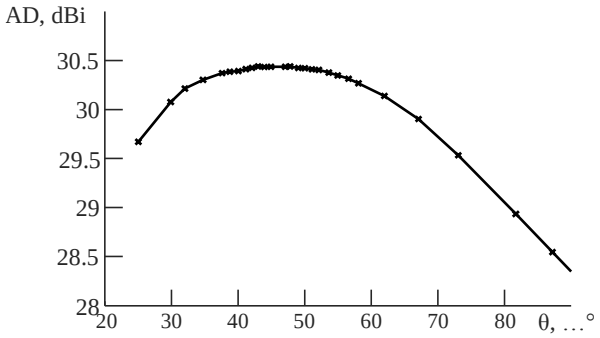

Fig. 5. ILA AD dependence on the primary feed RP width

AD does not depend on the lens size, but only on its material; consequently, the results are valid for lenses of any size (having a diameter of more than 5–10 wavelengths in a free-space) and can be used for further calculations.

Waveguide-based primary radiators are the most suitable means for controlling the radiation pattern width through a determination of the waveguide radiating opening dimensions [23]. An important aspect of the development of this radiator is the electrical coupling of the radiating waveguide aperture with an interface based on printed transmission lines for direct connection to radio frequency circuit elements. To solve this issue, an approach based on a microstrip antenna radiating in a waveguide channel, similar to that used in a number of waveguide-to-microstrip transitions, is used [28]–[31].

The designed ILA primary feed is based on a combination of the microstrip antenna and waveguide adapter with a square aperture of 8.5×8.5 mm that is optimised for implementation with a dielectric lens in the frequency band of 27.5…29.5 GHz. The structure and model of the designed primary feed are shown in Fig. 6.

The primary feed is implemented on a printed circuit board consisting of five dielectric layers and 6 metal levels. A high-frequency Rogers RO4350B (dielectric constant is $\varepsilon=3.66$) with a Rogers RO4450B ($\varepsilon=3.55$) prepreg laminate is chosen as a printed circuit board material. The main microstrip antenna radiating element is a square patch. The orthogonal linear polarisations are excited through the corresponding "H-type" slots in one of the internal metallisation levels of the printed circuit board (Fig. 6, *b*). The signal is fed by microstrip lines from the printed circuit board side opposite to the radiator, which allows isolating the radiating element from the radio frequency circuit elements of the communication system. The remaining board metallisation layers are not involved in a microstrip antenna structure formation. They are designed for the further transceiver board active circuits tracing.

The waveguide adapter, which is attached between the printed circuit board and the lens, corrects the patch radiation by optimising the dimensions of its radiating opening, allowing the lens surface to be uniformly illuminated and leading to a corresponding increase in ILA AG.

Fig. 6, *a* shows the adapter aperture containing a matching dielectric insert of a circular cross-section having a diameter of 3 mm and a height of 4.6 mm. Technologically, such an insert is fabricated as a protrusion of a flat lens base at the adapter attachment point, serving to improve the dielectric lens and match the impedance of the waveguide adapter [23].

Electromagnetic simulation of the designed ILA primary feed is carried out in the computer-aided design (CAD) system CST Microwave Studio. In the full-wave simulation, dielectric material losses of a printed circuit board are taken into account based on the experimental data reported in [32], [33]. In particular, the dielectric loss tangent is taken equal to

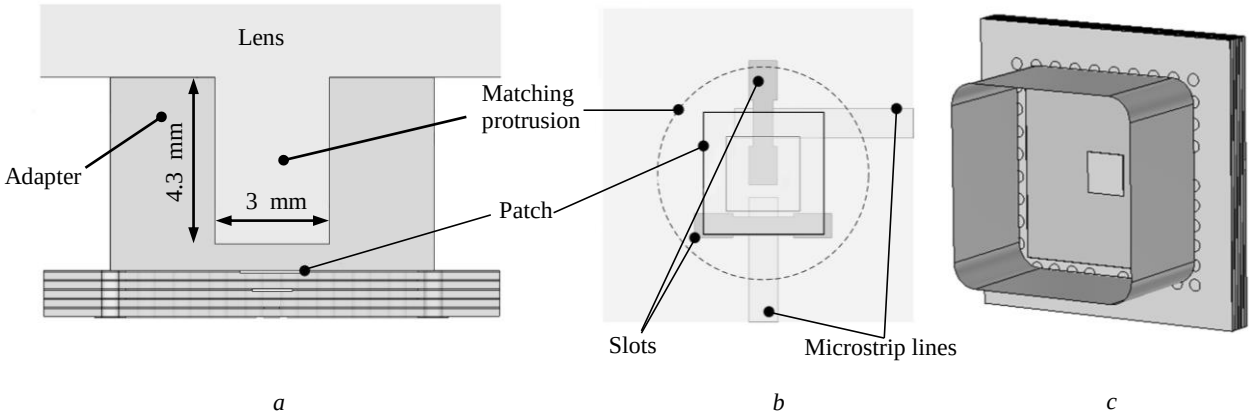

Fig. 6. Cross-section structure of the primary feed with adapter (*a*); single microstrip antenna structure (*b*); primary feed model (*c*)

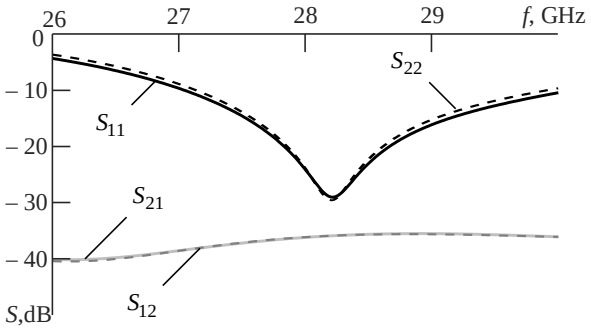

Fig. 7. The designed primary feed electrodynamic modelling results

0.005 in the whole studied frequency band of 27.5…29.5 GHz. In addition, the simulation accounts losses in metal conductors by specifying the total conductivity and roughness of the copper foil.

The results of the primary feed *S*-parameters simulation are shown in Fig. 7. It is noted that the surrounding space boundary conditions and parameters are set to provide the primary feed radiation into the medium (half space) with the dielectric lens material parameters that allows the designed primary feed parameters inside the lens body to be determined.

In accordance with simulation results, the designed primary feed provides a reflection coefficient level for each of the ports corresponding to two polarisations S_{11} and $S_{22} < -13$ dB in the whole system operating frequency band of 27.5…29.5 GHz. The polarisation isolation level within the band is more than 35 dB.

In the lens body, the primary feed provides radiation patterns that are similar in shape to each polarisation with the gain of 10.8…11.5 dBi and radiation efficiency of at least 96% (no less than 0.2 dB) in the whole frequency band of 27.5…29.5 GHz. Radiation pattern cross-sections in the dielectric lens body obtained with the simulation results while designed primary feed orthogonal ports excitation at the centre frequency of 28.5 GHz are shown in Fig. 8. The cross-sections are presented in two principal planes ($\phi = 0°$ (solid lines) and $\phi = 90°$ (dashed lines)). A black colour denotes port 1, while a grey colour denotes port 2.

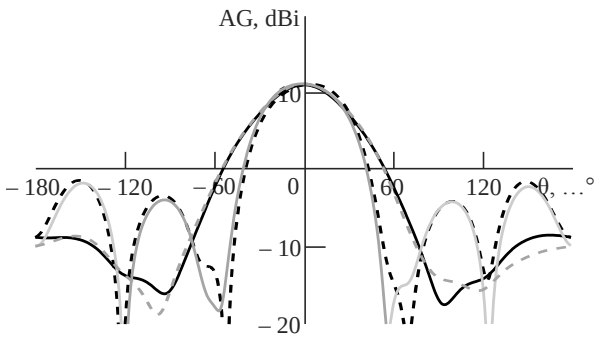

Fig. 8. Radiation pattern cross sections of the primary feed in the dielectric lens body

According to the simulation results, the primary feed forms a radiation pattern in the lens body having a half-power beamwidth of 47…51° for both orthogonal polarisations, which is within optimum values to achieve the required ILA AG values (Fig. 5).

Experimental study of the prototype. The elements of the designed lens antenna having a dual-polarised primary feed were constructed for experimental studies. Probe-type waveguide-to-microstrip transitions with waveguide plugs were added to the printed circuit board structure to allow the connection of measurement equipment having a standard waveguide interface WR-28 to the microstrip lines of the designed primary feed [31]. In order to take into account the effects of transitions and supply microstrip lines on the characteristics of dual-polarised ILAs, these were primarily tested using back-to-back ("waveguide–microstrip line–waveguide") transitions (Fig. 9). The printed circuit board structure with test elements is completely identical to the board structure used for the planar primary feed.

Specific path losses in the microstrip line allow back-to-back test elements having different microstrip line lengths (15 and 25 mm) to be experimentally estimated and thus taken into account when determining the characteristics of individual transitions and the designed ILA. Transitions provide a reflection coefficient level $S_{11} < -20$ dB in the considered frequency band of 27.5…29.5 GHz. In this case, an individual transition loss is no more than 0.4 dB, while the pathloss specific to the microstrip line does not exceed 0.7 dB/cm.

Photographs of the printed circuit board with a planar dual-polarised primary feed and waveguide-to-microstrip transitions are shown in Fig. 10, *a* and *b*.

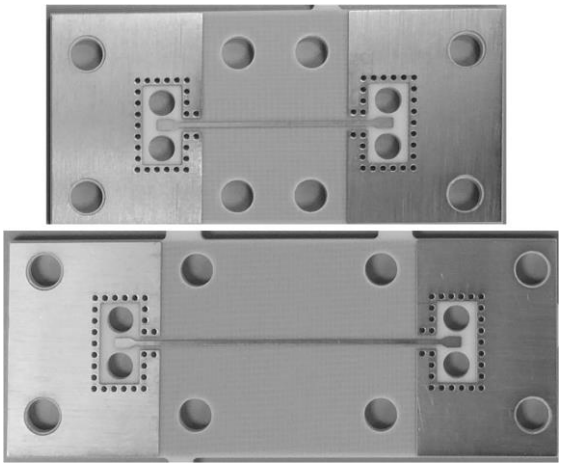

Fig. 9. Back-to-back waveguide-microstrip line-waveguide structures for testing the of the waveguide-to-microstrip transition characteristics

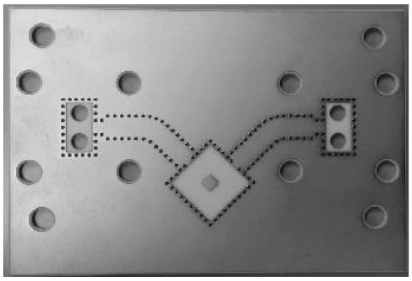

a

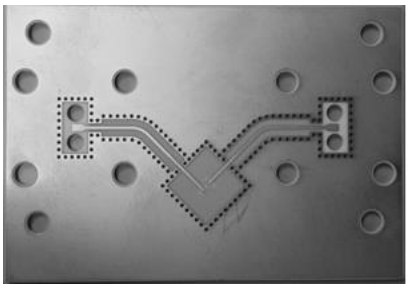

b

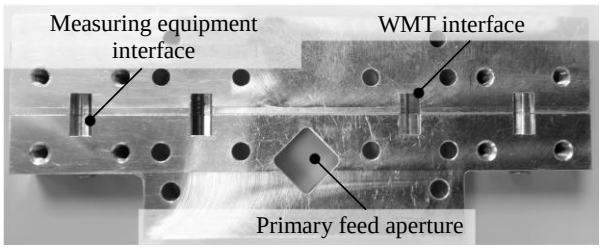

c

Fig. 10. Photos: *a* – top view of the printed circuit board with dual-polarized primary feed; *b* – bottom view of the printed circuit board with dual-polarized primary feed; *c* –waveguide adapter

The waveguide adapter photo is shown in Fig. 10, *c*. The adapter contains the primary feed waveguide aperture and waveguide channels based on a rectangular waveguide of standard cross-section WR-28, which is used to simplify the connection of measuring equipment. The adapter is divided into 2 parts that connect in the middle of the waveguide channel to allow a waveguide channel to be manufactured by milling. In this case, the waveguide channel turns out to be divided in an *E*-plane along which the electric current density is minimal, and slots due to metal elements conjugation do not significantly affect the waveguide characteristics.

A specially-designed polarisation insert is used to measure losses in the dual-polarised ILA feed system (Fig. 11). This insert is attached to the adapter antenna port instead of the lens in such a way that a wide wall of its rectangular aperture is perpendicular to one of the primary feed supply lines. The adapter is matched to this microstrip line according to the reflection coefficients and the corresponding polarisation of the radiating patch. Additionally, for orthogonal linear polarisation signals, such an insert is fully reflective.

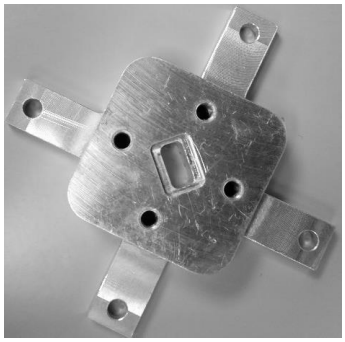

Fig. 11. Polarising insert

A comparison of the simulation results (solid line) and measurements (dashed line) of the primary feed with distribution system is shown in Fig. 12 (black lines correspond to Port 1, while grey lines denote Port 2). The distribution system (up to antenna port) losses are 1.8…2 dB. Thus, without losses in waveguide-to-microstrip transitions and feed lines, which were previously estimated when measuring two-sided test structures, the designed primary feed together with the adapter introduces losses of less than 0.4 dB.

Fig. 13 shows a photo of a manufactured dielectric lens with a diameter of D = 120 mm. The weight

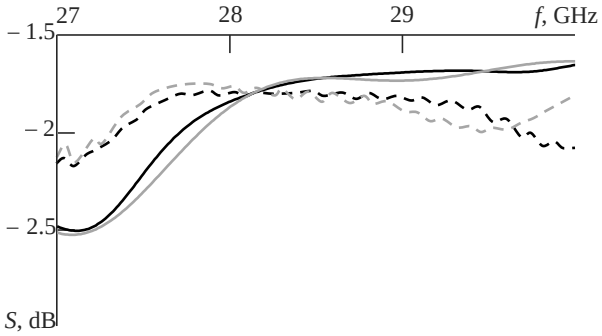

Fig. 12. Feed system insertion losses

Fig. 13. Dielectric lens

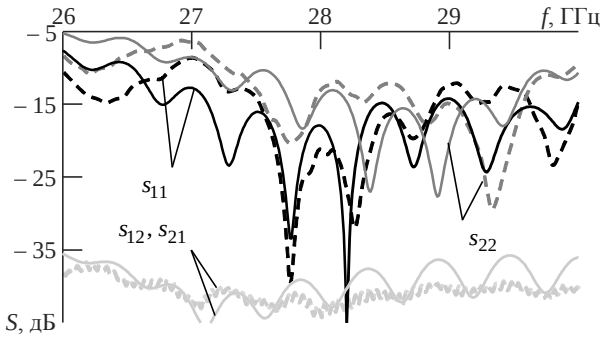

Fig. 14. Comparison of simulated and measured S-parameters of ILA

of the manufactured lens is 1.1 kg. The lens cylindrical extension is modified to facilitate attachment of the adapter and secure its fixation in the measurement setup. For this purpose, special screw-threaded inserts are installed in blind holes manufactured on the lens base. A matching protrusion with the dimensions shown in Fig. 6, *a* is implemented on the flat lens base.

Antenna *S*-parameters are measured by using a vector network analyser Keysight N5224A PNA. During measurements, network analyser ports are connected to the corresponding signal feed system input waveguide interfaces by using high-quality coaxial cables, which have low internal losses combined with waveguide-coaxial transitions, manufactured by Mi-Wave company. The ILA was placed on a stand with a radio absorbing material (RAM) to eliminate reflections from the surrounding area. A comparison of the measured (dashed lines) and obtained by electrodynamic simulation (solid) lens antenna *S*-parameters is shown in Fig. 14.

S-parameters frequency dependences have oscillations that are absent in the individual primary feed simulation results. These oscillations are caused by radiation reflections from the inner elliptical lens surface, which return to the ellipse focus where the primary feed is located in accordance with the principles of geometric optics. These oscillations do not lead to changes in the average reflection and isolation coefficient values. From the presented data, it is clear that a good agreement between the full-wave simulation and measurements results has been achieved. The antenna provides an isolation level between cross-polarised ports of more than 37 dB and a reflection coefficients value S_{11} S_{22} of no more than –12 dB in the frequency band of 27.5…29.5 GHz.

The measurement setup is used to measure AG and radiation pattern of the dual-polarised lens antenna (Fig. 15).

During measurement, the lens antenna was fixed in a special holding device located on a software-controlled rotary positioner. The distance between the receiving (standard horn antenna) and transmitting (ILA) antennas is set at 3.5 m in order to meet the far field requirement. The receiving horn antenna is built into a RAM screen slit to eliminate the influence of room reflections and thereby increase measurement accuracy.

The ILA radiation pattern measurements are carried out separately for each of the orthogonal ports in *E*- and *H*-planes at three key frequencies (27.5, 28.5 and 29.5 GHz). In this case, an unused antenna port is connected to a matched waveguide load. Fig. 16 shows the measured (dashed lines) and obtained by full-wave simulation (solid lines) ILA radiation patterns corresponding to orthogonal polarisations at a centre frequency of 28.5 GHz for two ports (black lines denote *E*-plane, grey denotes *H*-plane).

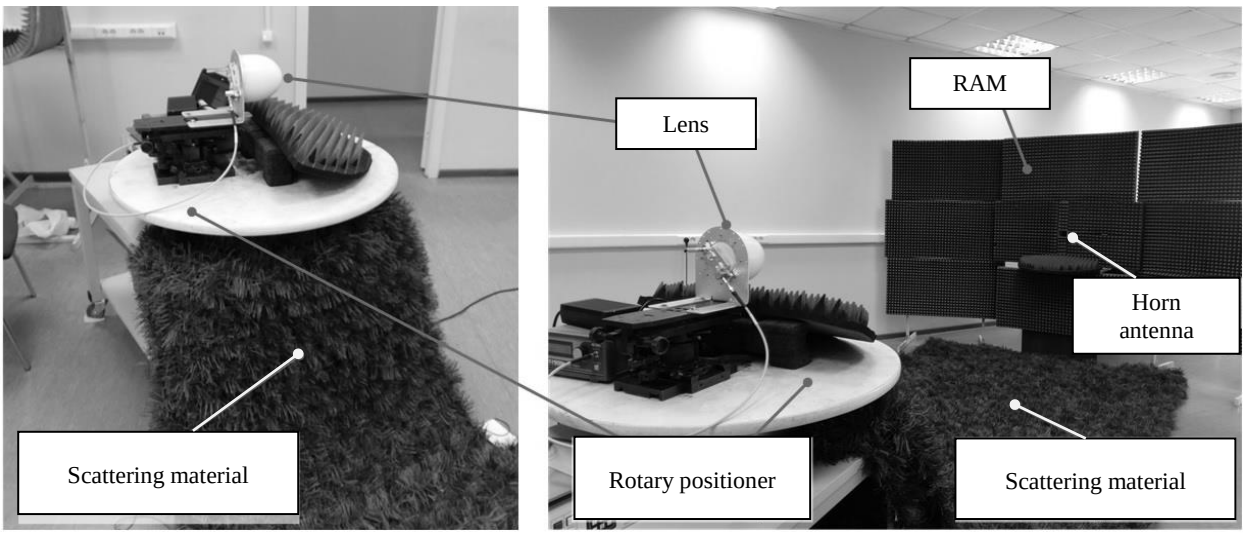

Fig. 15. Antenna measurement setup

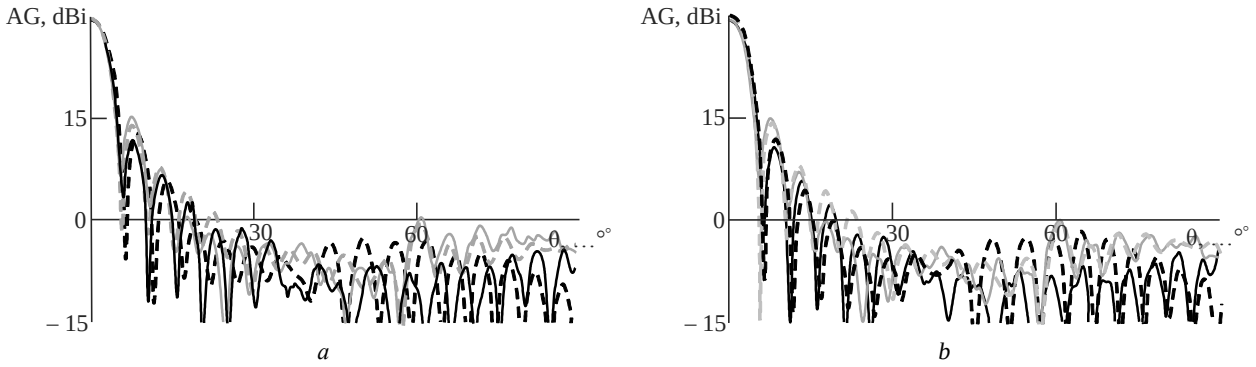

a *b*

Fig. 16. Measured and modelled radiation patterns for port 1 (*a*) and port 2 (*b*)

Table 1. Radiation pattern parameters of the designed ILA

f, GHz		Beam width, …°	Gain, dBi
Port 1	27.5	5.1 (5.1)	29.8 (29.8)
	28.5	4.8 (4.9)	30.2 (30.2)
	29.5	4.8 (4.8)	29.9 (30.3)
Port 2	27.5	5.1 (5.1)	29.5 (29.7)
	28.5	4.8 (4.9)	29.8 (30.1)
	29.5	4.8 (4.8)	29.9 (30.3)

The results show a good agreement between the measured radiation patterns and those obtained with the full-wave simulation, both in the AG level and the main lobe and side lobe regions. Summary data of measured and simulated (results are shown in brackets) designed ILA parameters are presented in Table 1.

The measured AG values of the designed ILA, within 29.5…30.3 dBi for each polarisation, are in good agreement with the full-wave simulation results and preliminary estimations. At the same time, the measured aperture efficiency of the designed antenna is 71…79%, confirming the effectiveness of the illumination of ILA surface by the developed primary feed. The first side lobe level does not exceed –15 dB for each polarisation at all measured frequencies.

A comparison of the characteristics of the developed high gain dual-polarised ILA having different antenna designs as discussed in the introduction is presented in Table 2. It can be seen that the designed antenna surpasses other antennas in the frequency band of 27.5…29.5 GHz in terms of aggregate parameters and characteristics taking its operability on two orthogonal linear polarisations into account.

Conclusion. The results of the design, full-wave simulation and measurements of the ILA having a planar dual-polarised primary feed, intended for use in fixed "point-to-point" and "point-to-multipoint" communication systems of the frequency band of 27.5…29.5 GHz, are presented. The antenna consists of a hemielliptical lens with a diameter of D = 120 mm, which is made of an HDPE having dielectric constant ε = 2.3 and a low dielectric loss tangent value in the considered frequency band, as well as a primary feed located on a flat lens base at the focal point. The designed ILA primary feed is based on a combination of the microstrip antenna and the waveguide adapter having a square aperture of 8.5×8.5 mm. The adapter aperture size is selected using an analytical method based on a combination of geometric and physical optics principles, allowing the ILA aperture efficiency – and, consequently, its AG – to be increased. The adapter aperture contains a dielectric matching insert of a circular cross-section

Table 2. Comparative table of the considered antennas parameters

Source of literature	Frequency range, GHz	Gain, dBi	Work on two polarizations	Printed Line Interface
Present work	27.5…29.5	29.5…30.3	Yes	Yes
[12]	28…32	22.5	No	Yes
[13]	26…30	19	Yes	Yes
[14]	12.25…12.75/ 14…14.5	33.7	Yes	Yes
[17]	26.9…29.2	22	No	Yes
[19]	23.5…25	20	Yes	Yes
[20]	23.5…24.5	17.5	No	No
[22]	24.3…24.7	20.5	No	Yes
[23]	25	32.5	No	Yes
[25]	27.5…29.5	23.5	Yes	No
[28]	34…36	34	Yes	No

on a flat lens base, which serves to improve the impedance matching of the dielectric lens and waveguide adapter.

According to the measurement results, the designed ILA in the frequency band of 27.5…29.5 GHz provides an AG level within 29.5…30.3 dBi for each polarisation, which is achieved due to its high aperture efficiency (71–79%) and small losses in the feed system. The main lobe half-power beamwidth is 4.8…5.1°, while the first side lobe level does not exceed –15 dB. The ILA signal feed system is made on the basis of microstrip transmission lines and provides impedance matching according to a reflection coefficient level of $S_{11} < -12$ дБ. The isolation level between the ILA orthogonal antenna ports is at least 37 dB.

The designed ILA can be successfully used in radio communication systems of the 27.5…29.5 GHz frequency range.

REFERENCES

1. Decision of The State Commission for Radio Frequencies 25.06.2007 no 07-21-01-001. About the use of radio frequency bands in the 1.5 GHz and 28 GHz bands by radio electronic means of fixed civil access for civilian use. Available at: http://www.rfs-rf.ru/upload/medialibrary/fc3/018816.doc (accessed: 22.02.2019) (In Russ.)

2. Recommendation ITU-R F.748-4 (05/2001). Radiofrequency arrangements for systems of the fixed service operating in the 25, 26 and 28 GHz bands. Available at: https://www.itu.int/dms_pubrec/itu-r/rec/f/R-REC-F.748-4-200105-I!!PDF-E.pdf (accessed: 22.02.2019)

3. Harmonised European Standard ETSI EN 302 326-3 V1.3.1 (2008-02). Fixed Radio Systems; Multipoint Equipment and Antennas; Part 3: Harmonised EN covering the essential requirements of article 3.2 of the R&TTE Directive for Multipoint Radio Antennas. Available at: https://www.etsi.org/deliver/etsi_en/302300_302399/30232603/01.03.01_60/en_30232603v010301p.pdf (accessed: 22.02.2019)

4. Rappaport T. S., Sun Sh., Maysus R., Zhao H., Azar Y., Wang K., Wong G. N., Schulz J. K., Samimi M., Gutierrez F. Millimetre Wave Mobile Communications for 5G Cellular: It Will Work! IEEE Access. 2013, vol. 1, no. 1, pp. 335–349. doi: 10.1109/ACCESS.2013.2260813

5. Wells J. Faster than fiber: The future of multi-G/s wireless. IEEE Microwave Magazine. 2009, vol. 10, iss. 3, pp. 104–112. doi: 10.1109/MMM.2009.932081

6. Al-Hourani A., Chandrasekharan S., Kandeepan S. Path loss study for millimetre wave device-to-device communications in urban environment. IEEE International Conference on Communications Workshops (ICC). 10-14 June 2014. Sydney, Australia. 2014. Piscataway, IEEE, pp. 102–107. doi: 10.1109/ICCW.2014.6881180

7. Recommendation ITU-R P.676-11 (09/2016) “Attenuation by atmospheric gases”. Available at: https://www.itu.int/dms_pubrec/itu-r/rec/p/R-REC-P.676-11-201609-I!!PDF-E.pdf (accessed: 22.02.2019)

8. Qingling Z., Li J. Rain Attenuation in Millimetre Wave Ranges. 7th Intern. Symp. on Antennas, Propagation and EM Theory. 26–29 Oct. 2006. Guilin, China. Piscataway, IEEE, 2006, pp. 1–4. doi: 10.1109/ISAPE.2006.353538

9. Recommendation ITU-R P.838-3 (03/2005). Specific attenuation model for rain for use in prediction methods. Available at: https://www.itu.int/dms_pubrec/itu-r/rec/p/R-REC-P.838-3-200503-I!!PDF-E.pdf (accessed: 22.02.2019)

10. Recommendation ITU-R P.837-7 (06/2017). Characteristics of precipitation for propagation modelling. Available at: https://www.itu.int/dms_pubrec/itu-r/rec/p/R-REC-P.837-7-201706-I!!PDF-E.pdf (accessed: 22.02.2019)

11. Boccardi F., Heath R. W., Lozano A., Marzetta T. L., Popovski P. Five Disruptive Technology Directions for 5G. IEEE Communications Magazine, 2014, vol. 52, iss. 2, pp. 74–80. doi: 10.1109/MCOM.2014.6736746

12. Kibaroglu K., Sayginer M., Phelps T., Rebeis G. M. A 64-Element 28-GHz Phased-Array Transceiver With 52-dBm EIRP and 8–12-Gb/s 5G Link at 300 Meters Without Any Calibration. IEEE Transactions on Microwave Theory and Techniques. 2018, vol. 66, iss. 12, pp. 5796–5811. doi: 10.1109/TMTT.2018.2854174

13. Churkin S., Mozharovskiy A., Artemenko A., Maslennikov R. Microstrip patch antenna arrays with fan-shaped 90 and 45-degree wide radiation patterns for 28 GHz MIMO applications. 12th European Conf. on Antennas and Propagation (EuCAP). 9-13 April 2018. London, UK. 2018, pp. 1–5. doi: 10.1049/cp.2018.1204

14. Ohtsuk M., Takahashi T., Konishi Y., Urasaki S., Harada K. A dual-polarised planar array antenna for Ku-band satellite communications. IEEE Antennas and Propagation Society International Symposium Digest. Antennas: Gateways to the Global Network. Held in conjunction with: USNC/URSI National Radio Science Meeting. 21–26 June 1998. Atlanta, USA. Piscataway, IEEE, 1998, pp. 16–19. doi: 10.1109/APS.1998.698732

15. Diawuo H. A., Jung Y.-B. Broadband Proximity-Coupled Microstrip Planar Antenna Array for 5G Cellular Applications. IEEE Antennas and Wireless Propagation Letters, 2018, vol. 17, iss. 7, pp. 1286–1290. doi: 10.1109/LAWP.2018.2842242

16. Hamberger G. F., Drexler A., Trummer S., Siart U., Eibert T. F. A planar dual-polarised microstrip 1D-beamforming antenna array for the 24GHz ISM-band. 10th European Conf. on Antennas and Propagation (EuCAP). 10-15 April 2016. Davos, Switzerland. Piscataway, IEEE, 2016, pp. 1–5. doi: 10.1109/EuCAP.2016.7481205

17. Zhang L., Li L., Yi H. Design of a Traveling Wave Slot Array on Substrate Integrated Waveguide for 24GHz Traffic Monitoring. Cross Strait Quad-Regional Radio Science and Wireless Technology Conference (CSQRWC). 21–24 July 2018. Xuzhou, China. Piscataway, IEEE, 2018, pp. 1–3. doi: 10.1109/CSQRWC.2018.8455559

18. Chang Y.-L., Jiao Y.-C., Zhang L., Chen G., Qiu X. A K-band series-fed microstip array antenna with low side-lobe for anticollision radar application. Sixth Asia-Pacific Conference on Antennas and Propagation (APCAP). 16-19 Oct. 2017. Xi'an, China. Piscataway, IEEE, 2017, pp. 1–3. doi: 10.1109/APCAP.2017.8420878

19. Sakakibara K., Shida K., Mouri Y., Kikuma N. Centre-fed traveling-wave microstrip array antenna using elliptically-shaped radiating elements in quasi millimetre-wave band. IEEE International Symposium on Antennas and Propagation & USNC/URSI National Radio Science Meeting. 9-14 July 2017. San Diego, USA. Piscataway, IEEE, 2017, pp. 2609–2610. doi: 10.1109/APUSNCURSINRSM.2017.8073347

20. Mozharovskiy A., Churkin S., Artemenko A., Maslennikov R. 28 GHz waveguide antennas with fan-shaped patterns for base stations MIMO applications. 12th European Conference on Antennas and Propagation (EuCAP). 9-13 April 2018. London, UK. 2018, pp. 1–5. doi: 10.1049/cp.2018.0373

21. Dufilie P. A. A Ka-band Dual-Pol Monopulse Shaped Reflector Antenna. IEEE International Symposium on Antennas and Propagation and USNC/URSI National Radio Science Meeting. 8-13 July 2018. Boston, USA. Piscataway, IEEE, 2018, pp. 1717–1718. doi: 10.1109/APUSNCURSINRSM.2018.8608180

22. Filipovic D. F., Gearhart S. S., Rebeis G. M. Double-Slot Antennas on Extended Hemispherical and Elliptical Silicon Dielectric Lenses. IEEE Transactions on Microwave Theory and Techniques. 1993, vol. 41, no. 10, pp. 1738–1749. doi: 10.1109/22.247919

23. Artemenko A., Maltsev A., Mozharovskiy A., Sevastyanov A., Ssorin V. Millimetre-Wave Electronically Steerable Integrated Lens Antennas for WLAN/WPAN Applications. IEEE Transactions on Antennas Propagation. 2013, vol. 61, pp. 1665–1671. doi: 10.1109/TAP.2012.2232266

24. Mozharovskiy A., Artemenko A., Ssorin V., Maslennikov R., Sevastyanov A. High gain millimetre-wave lens antennas with improved aperture efficiency. 9th European Conference on Antennas and Propagation (EuCAP). 13-17 April 2015, Lisbon, Portugal. Piscataway, IEEE, 2015, pp. 1–5.

25. Boriskin A. V., Sauleau R., Nosich A. I. Performance of Hemielliptic Dielectric Lens Antennas With Optimal Edge Illumination. IEEE Transactions on Antennas Propagation. 2009, vol. 57, no. 7, pp. 2193–2198. doi: 10.1109/TAP.2009.2021979

26. Golub' V. D., Myskov A. S., Mozharovskii A. V., Artemenko A. A., Maslennikov R. O. *Razrabotka i optimisatsiya antennoi reshetki obluchatelei dlya skaniruyushchei linzovoi antenny chastotnogo diapazona 71–76 GGts* [Development and optimisation of the antenna array of irradiators for a scanning lens antenna of the frequency range 71-76 GHz]. Conference Proc. Antennas and the Distribution of Radio Waves. St. Petersburg, 2018, pp. 112–116 (In Russ.)

27. Mozharovskii A. V., Artemenko A. A., Mal'tsev A. A., Maslennikov R. O., Sevast'yanov A. G., Ssorin V. N. An effective method for calculating the characteristics of integrated lens antennas based on geometrical and physical optical approximations. Radiophysics and Quantum Electronics. 2015, vol. 58, no. 6, pp. 492–504. (In Russ.)

28. Lee H. Y., Jun D. S., Moon S. E., Kim E. K., Park J. H., Park K. H. Wideband aperture coupled stacked patch type microstrip to waveguide transition for V-band. IEEE Proc. of Asia-Pacific Microwave Conf. 12-15 Dec. 2006. Yokohama, Japan. Picataway, IEEE, 2006, pp. 360–362. doi: 10.1109/APMC.2006.4429440

29. Artemenko A. A., Maslennikov R. O., Sevast'yanov A. G., Ssorin V. N. *Volnovodno-mikropoloskovyi perekhod v chastotnom diapazone 60 GGts* [Waveguide-microstrip junction in the 60 GHz frequency range]. 19th Intern. Crimean Conf. Microwave Engineering and Telecommunication Technologies, 2009, pp. 505–506. (In Russ.)

30. Artemenko A., Maltsev A. , Maslennikov R., Sevastyanov A., Ssorin V. Design of wideband waveguide to microstrip transition for 60 GHz frequency band. Proc. of 41st European Microwave Conf. (EuMC). 10-13 Oct. 2011. Manchester, UK. Piscataway, IEEE, 2011, pp. 838–841. doi: 10.23919/EuMC.2011.6101966

31. Soykin O., Artemenko A., Ssorin V., Mozharovskiy A., Maslennikov R. Wideband Probe-Type Waveguide-to-Microstrip Transition for V-band Applications. Proc. of 46th European Microwave Conf. (EuMC). 4-6 Oct. 2016. London, UK. Piscataway, IEEE, 2016, pp. 1–4. doi: 10.1109/EuMC.2016.7824262

32. Felbecker R., Keusgen W., Peter M. Estimation of Permittivity and Loss Tangent of High Frequency Materials in the Millimetre Wave. IEEE Intern. Conf. on Microwaves, Communications, Antennas and Electronics Systems (COMCAS). 7-9 Nov. 2011. Tel Aviv, Israel. Piscataway, IEEE, 2011, pp. 1–8. doi: 10.1109/COMCAS.2011.6105829

33. Horn A. Dielectric constant and loss of selected grades of Rogers high frequency circuit substrates from 1-50 GHz. Rogers Corporation Technical Report 5788, 2003.

Andrey V. Mozharovskiy Engineer (2011) in Information Systems and Technologies (Lobachevsky State University of Nizhny Novgorod). Doctoral candidate of the Department of micro radio electronics and radio technology of Saint Petersburg Electro-technical University "LETI". Senior microwave systems and antennas engineer in LLC "Radio Gigabit". The author of 27 scientific publications. Area of expertise: various millimetre wavelength range antenna and feeding systems, including printed, waveguide and lens antennas and antenna arrays; planar and waveguide duplexing devices and filters.
E-mail: andrey.mozharovskiy@radiogigabit.com
https://orcid.org/0000-0002-9827-6720

СПИСОК ЛИТЕРАТУРЫ

1. Решение ГКРЧ от 25.06.2007 № 07-21-01-001 "Об использовании полос радиочастот в диапазонах 1.5 ГГц и 28 ГГц радиоэлектронными средствами фиксированного беспроводного доступа гражданского назначения" (в ред. от 16.04.2014 № 14-23-09-2). URL: http://www.rfs-rf.ru/upload/medialibrary/fc3/018816.doc (дата обращения 22.02.2019)

2. Recommendation ITU-R F.748-4 (05/2001). Radio-frequency arrangements for systems of the fixed service operating in the 25, 26 and 28 GHz bands. URL: https://www.itu.int/dms_pubrec/itu-r/rec/f/R-REC-F.748-4-200105-I!!PDF-E.pdf (дата обращения 22.02.2019)

3. Harmonised European Standard ETSI EN 302 326-3 V1.3.1 (2008-02). Fixed Radio Systems; Multipoint Equipment and Antennas; Part 3: Harmonised EN covering the essential requirements of article 3.2 of the R&TTE Directive for Multipoint Radio Antennas. URL: https://www.etsi.org/deliver/etsi_en/302300_302399/30232603/01.03.01_60/en_30232603v010301p.pdf (дата обращения 22.02.2019)

4. Millimetre Wave Mobile Communications for 5G Cellular: It Will Work! / T. S. Rappaport, Sh. Sun, R. Maysus, H. Zhao, Y. Azar, K. Wang, G. N. Wong, J. K. Schulz, M. Samimi, F. Gutierrez // IEEE Access. 2013. Vol. 1, № 1. P. 335–349. doi: 10.1109/ACCESS.2013.2260813

5. Wells J. Faster than fiber: The future of multi-G/s wireless // IEEE Microwave Magazine. 2009. Vol. 10, iss. 3. P. 104–112. doi: 10.1109/MMM.2009.932081

6. Al-Hourani A., Chandrasekharan S., Kandeepan S. Path loss study for millimetre wave device-to-device communications in urban environment // IEEE Intern. Conf. on Communications Workshops (ICC), Sydney, Australia, 10–14 June 2014. Piscataway: IEEE. P. 102–107. doi: 10.1109/ICCW.2014.6881180

7. Recommendation ITU-R P.676-11 (09/2016) "Attenuation by atmospheric gases". URL: https://www.itu.int/dms_pubrec/itu-r/rec/p/R-REC-P.676-11-201609-I!!PDF-E.pdf (дата обращения 22.02.2019)

8. Qingling Z., Li J. Rain Attenuation in Millimetre Wave Ranges // 7th Intern. Symp. on Antennas, Propagation and EM Theory, Guilin, China, 26–29 Oct. 2006. Piscataway: IEEE, 2006. P. 1–4. doi: 10.1109/ISAPE.2006.353538

9. Recommendation ITU-R P.838-3 (03/2005). Specific attenuation model for rain for use in prediction methods. URL: https://www.itu.int/dms_pubrec/itu-r/rec/p/R-REC-P.838-3-200503-I!!PDF-E.pdf (дата обращения 22.02.2019)

10. Recommendation ITU-R P.837-7 (06/2017). Characteristics of precipitation for propagation modelling. URL: https://www.itu.int/dms_pubrec/itu-r/rec/p/R-REC-P.837-7-201706-I!!PDF-E.pdf (дата обращения 22.02.2019)

11. Five Disruptive Technology Directions for 5G / F. Boccardi, R. W. Heath, A. Lozano, T. L. Marzetta, P. Popovski // IEEE Communications Magazine. 2014. Vol. 52, iss. 2. P. 74–80. doi: 10.1109/MCOM.2014.6736746

12. A 64-Element 28-GHz Phased-Array Transceiver With 52-dBm EIRP and 8–12-Gb/s 5G Link at 300 Meters Without Any Calibration / K. Kibaroglu, M. Sayginer, T. Phelps, G. M. Rebeis // IEEE Transactions on Microwave Theory and Techniques. 2018. Vol. 66, iss. 12. P. 5796–5811. doi: 10.1109/TMTT.2018.2854174

13. Microstrip patch antenna arrays with fan-shaped 90 and 45-degree wide radiation patterns for 28 GHz MIMO applications / S. Churkin, A. Mozharovskiy, A. Artemenko, R. Maslennikov // 12th European Conf. on Antennas and Propagation (EuCAP), London, UK, 9–13 April 2018. P. 1–5. doi: 10.1049/cp.2018.1204

14. A dual-polarised planar array antenna for Ku-band satellite communications / M. Ohtsuk, T. Takahashi, Y. Konishi, S. Urasaki, K. Harada // IEEE Antennas and Propagation Society International Symposium Digest. Antennas: Gateways to the Global Network. Held in conjunction with: USNC/URSI National Radio Science Meeting, Atlanta, USA, 21–26 June 1998. Piscataway: IEEE, 1998. P. 16–19. doi: 10.1109/APS.1998.698732

15. Diawuo H. A., Jung Y.-B. Broadband Proximity-Coupled Microstrip Planar Antenna Array for 5G Cellular Applications // IEEE Antennas and Wireless Propagation Letters. 2018. Vol. 17, iss. 7. P. 1286–1290. doi: 10.1109/LAWP.2018.2842242

16. A planar dual-polarised microstrip 1D-beamforming antenna array for the 24GHz ISM-band / G. F. Hamberger, A. Drexler, S. Trummer, U. Siart, T. F. Eibert // 10th European Conf. on Antennas and Propa-

gation (EuCAP), Davos, Switzerland, 10–15 April 2016. Piscataway: IEEE, 2016. P. 1–5. doi: 10.1109/EuCAP.2016.7481205

17. Zhang L., Li L., Yi H. Design of a Traveling Wave Slot Array on Substrate Integrated Waveguide for 24GHz Traffic Monitoring // Cross Strait Quad-Regional Radio Science and Wireless Technology Conf. (CSQRWC), Xuzhou, China, 21–24 July 2018. Piscataway: IEEE, 2018. P. 1–3. doi: 10.1109/CSQRWC.2018.8455559

18. A K-band series-fed microstip array antenna with low sidelobe for anticollision radar application / Y.-L. Chang, Y.-C. Jiao, L. Zhang, G. Chen, X. Qiu // Sixth Asia-Pacific Conf. on Antennas and Propagation (APCAP), Xi'an, China, 16–19 Oct. 2017. Piscataway: IEEE, 2017. P. 1–3. doi: 10.1109/APCAP.2017.8420878

19. Centre-fed traveling-wave microstrip array antenna using elliptically-shaped radiating elements in quasi millimetre-wave band / K. Sakakibara, K. Shida, Y. Mouri, N. Kikuma // IEEE Intern. Symp. on Antennas and Propagation & USNC/URSI National Radio Science Meeting, San Diego, USA, 9–14 July 2017. Piscataway: IEEE, 2017. P. 2609–2610. doi: 10.1109/APUSNCURSINRSM.2017.8073347

20. 28 GHz waveguide antennas with fan-shaped patterns for base stations MIMO applications / A. Mozharovskiy, S. Churkin, A. Artemenko, R. Maslennikov // 12th European Conf. on Antennas and Propagation (EuCAP), London, UK, 9–13 April 2018. P. 1–5. doi: 10.1049/cp.2018.0373

21. Dufilie P. A. A Ka-band Dual-Pol Monopulse Shaped Reflector Antenna // IEEE Intern. Symp. on Antennas and Propagation and USNC/URSI National Radio Science Meeting, Boston, USA, 8–13 July 2018. Piscataway: IEEE, 2018. P. 1717–1718. doi: 10.1109/APUSNCURSINRSM.2018.8608180

22. Filipovic D. F., Gearhart S. S., Rebeis G. M. Double-Slot Antennas on Extended Hemispherical and Elliptical Silicon Dielectric Lenses // IEEE Transactions on Microwave Theory and Techniques. 1993. Vol. 41, № 10. P. 1738–1749. doi: 10.1109/22.247919

23. Millimetre-Wave Electronically Steerable Integrated Lens Antennas for WLAN/WPAN Applications / A. Artemenko, A. Maltsev, A. Mozharovskiy, A. Sevastyanov, V. Ssorin // IEEE Transactions on Antennas Propagation. 2013. Vol. 61. P. 1665–1671. doi: 10.1109/TAP.2012.2232266

24. High gain millimetre-wave lens antennas with improved aperture efficiency / A. Mozharovskiy, A. Artemenko, V. Ssorin, R. Maslennikov, A. Sevastyanov // 9th European Conf. on Antennas and Propagation (EuCAP), Lisbon, Portugal, 13–17 April 2015. Piscataway: IEEE, 2015. P. 1–5.

25. Boriskin A. V., Sauleau R., Nosich A. I. Performance of Hemielliptic Dielectric Lens Antennas With Optimal Edge Illumination // IEEE Transactions on Antennas Propagation. 2009. Vol. 57, № 7. P. 2193–2198. doi: 10.1109/TAP.2009.2021979

26. Разработка и оптимизация антенной решетки облучателей для сканирующей линзовой антенны частотного диапазона 71–76 ГГц / В. Д. Голубь, А. С. Мысков, А. В. Можаровский, А. А. Артеменко, Р. О. Масленников // Тр. конф. “Антенны и распространение радиоволн”. СПб., 2018. С. 112–116.

27. Эффективный метод расчета характеристик интегрированных линзовых антенн на основе приближений геометрической и физической оптик / А. В. Можаровский, А. А. Артеменко, А. А. Мальцев, Р. О. Масленников, А. Г. Севастьянов, В. Н. Ссорин // Изв. вузов. Радиофизика. 2015. Т. 58, № 6. С. 492–504.

28. Wideband aperture coupled stacked patch type microstrip to waveguide transition for V-band / H. Y. Lee, D. S. Jun, S. E. Moon, E. K. Kim, J. H. Park, K. H. Park // IEEE Proc. of Asia-Pacific Microwave Conf., Yokohama, Japan, 12–15 Dec. 2006. Picataway: IEEE, 2006. P. 360–362. doi: 10.1109/APMC.2006.4429440

29. Волноводно-микрополосковый переход в частотном диапазоне 60 ГГц / А. А. Артеменко, Р. О. Масленников, А. Г. Севастьянов, В. Н. Ссорин // 19-я Междунар. Крымская конф. “СВЧ–техника и телекоммуникационные технологии”, 2009. С. 505–506.

30. Design of wideband waveguide to microstrip transition for 60 GHz frequency band / A. Artemenko, A. Maltsev, R. Maslennikov, A. Sevastyanov, V. Ssorin // Proc. of 41st European Microwave Conf. (EuMC), Manchester, UK, 10–13 Oct. 2011. Piscataway: IEEE, 2011. P. 838–841. doi: 10.23919/EuMC.2011.6101966

31. Wideband Probe-Type Waveguide-to-Microstrip Transition for V-band Applications / O. Soykin, A. Artemenko, V. Ssorin, A. Mozharovskiy, R. Maslennikov // Proc. of 46th European Microwave Conf. (EuMC), London, UK, 4–6 Oct. 2016. Piscataway: IEEE, 2016. P. 1–4. doi: 10.1109/EuMC.2016.7824262

32. Felbecker R., Keusgen W., Peter M. Estimation of Permittivity and Loss Tangent of High Frequency Materials in the Millimetre Wave // IEEE Intern. Conf. on Microwaves, Communications, Antennas and Electronics Systems (COMCAS), Tel Aviv, Israel, 7–9 Nov. 2011. Piscataway: IEEE, 2011. P. 1–8. doi: 10.1109/COMCAS.2011.6105829

33. Horn A. Dielectric constant and loss of selected grades of Rogers high frequency circuit substrates from 1-50 GHz. Rogers Corporation Technical Report 5788, 2003.

Можаровский Андрей Викторович – инженер (2011) по специальности “Информационные системы и технологии” (ННГУ им. Н. И. Лобачевского, г. Нижний Новгород). Соискатель кафедры микрорадиоэлектроники и технологии радиоаппаратуры Санкт-Петербургского государственного электротехнического университета “ЛЭТИ”. Старший инженер по СВЧ-устройствам и антенной технике ООО “Радио Гигабит”. Ав-

тор 27 научных публикаций. Сфера интересов – различные антенно-фидерные устройства миллиметрового диапазона длин волн, включая печатные, волноводные и линзовые антенны и антенные решетки; планарные и волноводные дуплексирующие устройства и фильтры.
E-mail: andrey.mozharovskiy@radiogigabit.com
https://orcid.org/0000-0002-9827-6720